Control Engineering Practice 76 (2018) 54–64

Contents lists available at ScienceDirect

Control Engineering Practice

journal homepage: www.elsevier.com/locate/conengprac

Robust autopilot design for landing a large civil aircraft in crosswind[☆]

Julian Theis[a,*], Daniel Ossmann[b], Frank Thielecke[a], Harald Pfifer[c]

[a] Institute of Aircraft Systems Engineering, Hamburg University of Technology, Hamburg, Germany
[b] Institute of System Dynamics and Control, German Aerospace Center (DLR) Oberpfaffenhofen, Wessling, Germany
[c] Mechanical Engineering Department, University of Nottingham, Nottingham, United Kingdom

ARTICLE INFO

Keywords:
Aircraft control
Flight control
Cascade control
Control design
Mixed sensitivity problem
H-infinity control

ABSTRACT

A comprehensive autolanding design for a representative model of a twin-engined commercial aircraft is presented in this paper. To facilitate the design task and minimize control law switching, a cascaded control structure is selected which resembles integrator chains. Classical loopshaping and robust control techniques are used to design the individual control loops. The emphasis is on providing a complete and comprehensive qualitative design strategy. The control system's ability to safely land the aircraft despite strong crosswind in a variety of possible scenarios is demonstrated in an industry-grade verification campaign. Nonlinear Monte Carlo simulations of the airliner model are used to assess the risk of unsafe landing conditions and provide insight into the performance characteristics and limitations of the proposed control system.

1. Introduction

Automatic control systems play a fundamental role in modern civil aviation and are by now capable of assisting the pilot in all flight segments. In fact, today's autopilots can perform challenging maneuvers such as to land the aircraft in poor visibility. To safely land the aircraft, the autopilot must achieve a very high level of precision in a variety of different scenarios. Crosswind poses one of the most severe dangers to landing aircraft. The autolanding system of the A320, e. g., is certified to perform safe landings in crosswind up to 20 knots. For comparison, the demonstrated crosswind in manual flight operation (that requires clear sight of the runway) on the A320 is 35 knots. Improving the ability to handle adverse wind conditions is thus important to increase performance and availability of future autolanding systems. Consequently, several researchers have investigated the potential of modern control techniques for this application, e. g., de Bruin & Jones, 2016; Holley & Bryson, 1977; Looye & Joos, 2006; Looye, Joos, & Willemsen, 2001; Shue & Agarwal, 1999. Others have focused on particular subtasks such as the "flare" maneuver immediately before touchdown, e. g., Biannic & Apkarian, 2001; Kaminer & Khargonekar, 1990; Navarro-Tapia, Simplicio, Iannelli, & Marcos, 2017.

The present article details the design of a complete autolanding system for the representative model of a twin-engined commercial transport aircraft in landing configuration. The airliner model was introduced by Biannic and Roos (2015) and is openly available from http://w3.onera.fr/smac/?q=aircraftModel. It was used in a design challenge formulated by Biannic and Boada-Bauxell (2016) from ONERA and Airbus in which the authors also participated (Theis, Ossmann, & Pfifer, 2017). The autopilot must steer the aircraft through the final approach starting 300 m above the runway all the way to touchdown. Available data to perform this task is based on current CAT-III instrument landing systems (ILS) and includes measurements of both vertical and horizontal deviation from the glide path. Success is defined as a gentle touchdown close to the runway centerline with wings level and landing gear aligned with the runway. The requirements are quantified by risk dispersions for the risk of short landing, long landing, hard landing, decentered landing, as well as landing with steep bank angle and landing with steep wheel sideslip angle. These dispersions are calculated through extensive Monte Carlo simulations over a wide range of environmental and system parameters.

The autopilot which is developed in the present article satisfies all requirements for 25 knots crosswind. This crosswind corresponds to the absolute maximum certification specification according to airworthiness code EASA CS-25.237. The design uses classical loopshaping and H_∞-norm optimal control. The required background information is provided in Section 2 and a problem formulation that facilitates easy tuning through physically relatable design parameters is developed. A cascaded control structure is proposed in Section 3 to resemble integrator chains.

☆ This research did not receive any specific grant from funding agencies in the public, commercial, or not-for-profit sectors.

* Corresponding author.
E-mail addresses: julian.theis@tuhh.de (J. Theis), daniel.ossmann@dlr.de (D. Ossmann), frank.thielecke@tuhh.de (F. Thielecke), harald.pfifer@nottingham.ac.uk (H. Pfifer).

https://doi.org/10.1016/j.conengprac.2018.04.010
Received 13 November 2017; Received in revised form 9 February 2018; Accepted 17 April 2018
0967-0661/

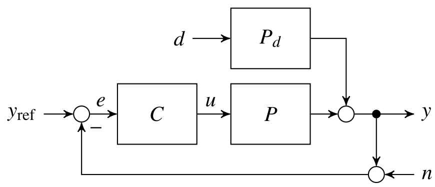

Fig. 1. Standard unity feedback loop.

This structure is different from the initial control design (Theis et al., 2017) and selected to make loopshaping design for the subsystems particularly easy. Comprehensive descriptions and insights on all subsystem design tasks are provided in Sections 4 and 5. Section 4 details the control system designs for the inner control loops using H_∞-norm optimal mixed sensitivity loopshaping. Section 5 details the design of the outer control loops through classical loopshaping. The complete design is evaluated in Section 6 in nonlinear Monte Carlo simulations, verifying robust performance.

2. Loopshaping control systems design

Let a linear time-invariant (LTI) plant model P, an LTI disturbance model P_d, and an LTI compensator C be given and arranged in the standard unity-feedback loop of Fig. 1. The output $y(t) \in \mathbb{R}^{n_y}$ collects all measurable signals used to calculate the control signal $u(t) \in \mathbb{R}^{n_u}$ and includes the effect of a disturbance $d(t) \in \mathbb{R}^{n_d}$ acting on the disturbance model. Additionally, the feedback signal is corrupted by measurement noise $n(t) \in \mathbb{R}^{n_y}$. In case only $n_r < n_y$ outputs are to be tracked, $y_{\text{ref}}(t) \in \mathbb{R}^{n_y}$ is without loss of generality taken as $y_{\text{ref}} = \left[\begin{smallmatrix} I_{n_r} \\ 0 \end{smallmatrix}\right] \bar{y}_{\text{ref}}$ with $\bar{y}_{\text{ref}}(t) \in \mathbb{R}^{n_r}$. The closed-loop transfer function governing this control loop are

$$y = \overbrace{(I + P\,C)^{-1} P\,C}^{T}\,(y_{\text{ref}} - n) + \overbrace{(I + P\,C)^{-1} P_d}^{S\,P_d}\; d \tag{1a}$$

$$u = \underbrace{C(I + P\,C)^{-1}}_{C\,S}\,(y_{\text{ref}} - n) - \underbrace{C(I + P\,C)^{-1} P_d}_{C\,S\,P_d}\; d. \tag{1b}$$

They are called the sensitivity $S = (I + P\,C)^{-1}$, control sensitivity $C\,S$, disturbance sensitivity $S\,P_d$, and complementary sensitivity $T := I - S = (I + P\,C)^{-1} P\,C$ (e. g. Skogestad & Postlethwaite, 2005).

Many properties of feedback control systems can be inferred from the magnitude of these sensitivity functions, e. g., disturbance attenuation levels, tracking capabilities, the frequency range of control activity, and robustness. In general, a control system should reduce the sensitivity S up to a specified frequency to improve disturbance rejection via $S\,P_d$. The relation $T = I - S$ further means that low sensitivity ($S \approx 0$) over a certain frequency range establishes tracking capabilities for reference signals as $T \approx I$ over this frequency range. The internal model principle (Francis & Wonham, 1975, 1976) can be used to derive desirable sensitivity functions for specific applications. For example, the requirement to follow setpoint changes in all output channels with zero steady-state error can be translated to a sensitivity function

$$S_{\text{ideal}} = \begin{bmatrix} \frac{s}{s+\omega_1} & & \\ & \ddots & \\ & & \frac{s}{s+\omega_{n_y}} \end{bmatrix}, \tag{2}$$

where ω_i, $i = 1, \ldots, n_y$ are the desired bandwidths for the individual channels of the multivariable control loop. That is, the ideal sensitivity function has zero steady-state gain, a slope of +20 dB per decade in each channel up to the desired bandwidth, and unit gain for higher frequencies. Such an ideal sensitivity is usually impossible to achieve due to Bode's sensitivity integral, as peak magnitude values of greater than 1 are the inevitable result of feedback (cf. Skogestad & Postlethwaite, 2005; Stein, 2003).

To improve transient behavior in response to a reference signal, two-degrees-of-freedom controllers are used. Such controllers consist of feedback (C_{FB}) and feedforward (C_{FF}) paths, i. e., the control signal is $u = C_{\text{FF}}\,\bar{y}_{\text{ref}} - C_{\text{FB}}\,y = K\left[\begin{smallmatrix} \bar{y}_{\text{ref}} \\ -y \end{smallmatrix}\right]$. In this case,

$$\begin{aligned} y = {} & \overbrace{(I + P\,C_{\text{FB}})^{-1} P\,C_{\text{FF}}}^{R}\;\bar{y}_{\text{ref}} \\ & - \overbrace{(I + P\,C_{\text{FB}})^{-1} P\,C_{\text{FB}}}^{T}\; n + \overbrace{(I + P\,C_{\text{FB}})^{-1} P_d}^{S\,P_d}\; d \end{aligned} \tag{3a}$$

$$\begin{aligned} u = {} & \underbrace{(I + C_{\text{FB}}\,P)\,C_{\text{FF}}}_{S_{\text{i}} C_{\text{FF}}}\;\bar{y}_{\text{ref}} \\ & - \underbrace{C_{\text{FB}}(I + P\,C_{\text{FB}})^{-1}}_{C_{\text{FB}} S}\; n - \underbrace{C_{\text{FB}}\,(I + P\,C_{\text{FB}})^{-1}\,P_d}_{C_{\text{FB}} S\,P_d}\; d. \end{aligned} \tag{3b}$$

Hence, reference tracking is governed by a reference transmission function R (n_y outputs and n_r inputs) which can be adjusted independently of the sensitivities. The error dynamics with respect to reference signals are described by the map $\left[\begin{smallmatrix} I_{n_r} \\ 0 \end{smallmatrix}\right] - R$, i. e., $e := y_{\text{ref}} - y = \left(\left[\begin{smallmatrix} I_{n_r} \\ 0 \end{smallmatrix}\right] - R\right)\bar{y}_{\text{ref}}$.

2.1. Classical loopshaping

A classical design technique for single-input-single-output systems is loopshaping [e. g. Horowitz 1963, Doyle, Francis, and Tannenbaum 1990]. It is based on "shaping" the looptransfer $L = P\,C$ such that desirable sensitivity functions are achieved. The ideal sensitivity function (2) translates to an ideal looptransfer $L_{\text{ideal}} = \frac{\omega}{s}$. Hence, the ideal compensator is $C_{\text{ideal}} = \frac{\omega}{s} P^{-1}$. It inverts the plant dynamics and adds integral action. Such a complete inversion is often neither possible nor desirable for reasons of control effort and robustness. Thus, the standard strategy is to select a compensator such the $\frac{\omega}{s}$-loopshape is approximately attained around the desired crossover frequency with sufficient gain in the low-frequency regime. This strategy is well-suited for model-based tuning of simple compensators such as proportional or proportional-integral controllers. It also proves useful for setting the bandwidth of cascaded control systems.

2.2. Mixed sensitivity loopshaping

Mixed sensitivity loopshaping (e. g. Skogestad & Postlethwaite, 2005; Zhou, Doyle, & Glover, 1995) seeks to directly shape sensitivity functions through weighted H_∞-norm optimization. The requirements are formulated in terms of weighting filters which specify a desired shape, e. g., low sensitivity at low frequencies. The plant model and the weights form a generalized closed-loop interconnection, G, and a controller can be found from the convex optimization problem

$$\min_{C_{\text{FB}}, C_{\text{FF}}} \|G(C_{\text{FB}}, C_{\text{FF}})\|_{H_\infty}. \tag{4}$$

This strategy is particularly useful for multivariable systems, where classical loopshaping is not applicable. Standard numerical tools exist to reliably solve (4), e. g., `hinfsyn` in Matlab's Robust Control toolbox which implements, among others, the formulation of Doyle, Glover, Khargonekar, and Francis (1989) and Glover and Doyle (1988). Controller tuning is performed by altering the weights.

The generalized closed-loop interconnection illustrated in Fig. 2 is proposed as a weighting scheme which is particularly easy to tune. It corresponds to the input–output map

$$\begin{aligned} \begin{bmatrix} z_1 \\ z_2 \end{bmatrix} = {} & \begin{bmatrix} W_e & 0 \\ 0 & W_u \end{bmatrix} \begin{bmatrix} D_e^{-1} & 0 \\ 0 & D_u^{-1} \end{bmatrix} \\ & \begin{bmatrix} S & S\,P_d & \left[\begin{smallmatrix} I \\ 0 \end{smallmatrix}\right] - R \\ C_{\text{FB}}\,S & C_{\text{FB}}\,S\,P_d & S_{\text{i}} C_{\text{FF}} \end{bmatrix} \begin{bmatrix} D_e & 0 & 0 \\ 0 & D_d & 0 \\ 0 & 0 & D_e^r \end{bmatrix} \begin{bmatrix} w_1 \\ w_2 \\ w_3 \end{bmatrix}. \end{aligned} \tag{5}$$